2022 13th International Symposium on Communication Systems, Networks and Digital Signal Processing (CSNDSP) | 978-1-6654-1044-1/22/$31.00 ©2022 IEEE | DOI: 10.1109/CSNDSP54353.2022.9907969

Design of MAC-layer Protocols for Distributed NOMA-based VLC Networks

Konstantinos G. Rallis*, Vasilis K. Papanikolaou*, Panagiotis D. Diamantoulakis*,
Alexis A. Dowhuszko†, Jyri Hämäläinen†, and George K. Karagiannidis*
*Department of Electrical and Computer Engineering, Aristotle University of Thessaloniki, GR-54124 Thessaloniki, Greece
†Department of Communications and Networking, Aalto University, 02150 Espoo, Finland
e-mails: konralgeo@ece.auth.gr, vpapanikk@auth.gr, padiaman@ieee.org,
alexis.dowhuszko@aalto.fi, jyri.hamalainen@aalto.fi, geokarag@auth.gr

***Abstract*—In this paper, a visible light communication (VLC) cellular network that utilizes non-orthogonal multiple access (NOMA) is investigated. To deal with the high inter-cell interference attributed to the high-density of VLC network nodes, a medium access control (MAC) scheduler is designed based on a distributed NOMA approach that aims at increasing the performance of cell-edge users, while securing the high data rate requirements of cell-center users in the VLC network. To this end, two practical protocols are proposed to guarantee the increased spectral efficiency and interference mitigation through distributed NOMA. In each protocol, the decoding strategy and power allocation of the users is investigated through a low complexity algorithm that ensures user fairness in the network. The presented analysis is validated through simulations, where the proposed schemes notably outperform the benchmark scheme in which the cell-edge user does not perform successive interference cancellation. Finally, the results showcase valuable insights, mainly on the fact that the decoding strategy in such networks is not as obvious as in conventional downlink NOMA.**

***Index Terms*—Visible Light Communication, Non-Orthogonal Multiple Access, decoding strategy, interference mitigation, distributed NOMA, successive interference cancellation.**

I. Introduction

Visible light communication (VLC) networks have attracted significant attention from the research community in the last decade, especially for providing indoor access, due to their widely available unlicensed bandwidth, ease of implementation thanks to the existing LED lightning infrastructure, robustness against strong Radio Frequency (RF) interference, and their inherent physical layer security [1], [2]. In order to fully explore the offered capabilities of VLC systems, techniques to address network coverage, multiple access, and interference mitigation should be designed and implemented with the particularities of such optical wireless networks in mind. On top of that, considerable attention has been given to non-orthogonal multiple access (NOMA), as it represents a popular method to increase the spectral efficiency of the network when compared, e.g., to conventional orthogonal multiple access schemes such as time-division multiple access (TDMA) [3]. NOMA for VLC networks has been extensively studied and showcased in the literature as an attractive candidate to secure high data rates and massive connectivity in indoor VLC networks [1], which are fundamental requirements to be fulfilled by the beyond 5G mobile standards that are being developed.

On the other hand, the high density and limited coverage area of a single VLC access point (AP) lead to the design of a wireless network based on the so-called attocell architecture. Due to the high density of transmission points, the VLC network has to deal with increased levels of inter-cell interference [4]. This can be combated, e.g., through network planning and frequency reuse patterns as proposed in various works [5]–[7]; however, such an approach introduces a cost in the overall spectral efficiency of the VLC network, which limits the benefit of ultra-densification. In this regard, coordinated multi-point (CoMP) transmission has been proposed as a framework for interference management, in order to enable the cooperation between adjacent VLC APs [8]. CoMP technology enables not only a reduction in the inter-cell interference power, but also a significant boost in the cell-edge user performance thanks to the improved received signal strength that is obtained. Recently, some NOMA-CoMP systems have been examined for conventional RF networks [9]–[11]. More specifically, the authors of [11] present a mutual successive interference cancellation (SIC) scheme to improve cell-edge user data rate and overall system throughput. On top of that, with the application of the distributed NOMA scheme, such as the one presented in [12], a VLC network can increase its ability to meet the target quality of service (QoS) of the users.

Motivated by this, a unified medium access control (MAC) scheduler is required to optimize the transmission and decoding strategy for each user in the network. Therefore, cell-edge users can be served by every AP whose coverage area includes them, aiming at mitigating the inter-cell interference power and, thus, achieving a higher spectral efficiency. For this purpose, the particularities of the VLC network such as the different optical wireless channel characteristics, capacity expressions, and constrains imposed by the VLC link must be examined. In this paper, we consider the case of two adjacent VLC attocells that serve three users, one of which is located in the area enclosed by the coverage areas of both APs. A unified MAC scheduler that utilizes distributed NOMA is employed to increase the cell-edge performance while searching for the optimal decoding strategy of each user. In this case, the QoS of the two users that are served by only

one AP, namely, the *strong* cell-center users, is guaranteed through a set of constraints, while the achievable rate of the third (cell-edge) user is maximized. In this case, we show that the optimal decoding strategy differs from the conventional downlink NOMA, in which the cell-center user is always the one performing SIC. Obtained simulation results identify various cases in which a different decoding strategy might be adopted by the users to obtain the optimal solution.

The rest of the paper is organized as follows: Section II presents the VLC-based system model and introduces the equations to implement the proposed the NOMA schemes. Section III derives the two algorithms that are proposed to schedule the transmission and decode the messages intended to the different users. Section IV shows the simulation parameters and the performance of the two proposed configurations, comparing them with benchmark scheme that does not use SIC in the cell-edge. Finally, conclusions are drawn in Section V.

II. System Model

A VLC network consisting of one central processing unit, two LED APs and three users is considered, as shown in Fig. 1. The coverage area of each AP is assumed to be a disk on the plane where the users are located. Due to the dense nature of the network, the coverage areas overlap in a common area. Each AP serves two users via cognitive radio (CR)-inspired NOMA [3]: one primary user in the non overlapping area and one secondary user in the common coverage area of both cells. Note that the secondary user is served simultaneously by both APs. Here, $i \in \mathcal{I} \triangleq \{1,2\}$ denotes the index of the VLC AP, whereas $j \in \mathcal{J} \triangleq \{1,2,3\}$ is the index of the user. Thus, as observed in Fig. 1, the channel gain between the j-th user who is served by the i-th AP at distance $d_{i,j}$ is given by

$$h_{i,j} = \frac{(m+1)}{2\pi d_{i,j}^2} A_r \cos^m(\phi_{i,j}) T(\psi_{i,j}) g(\psi_{i,j}) \cos(\psi_{i,j}), \quad (1)$$

where A_r is the sensitive area of the photodetector, $\phi_{i,j}$ and $\psi_{i,j}$ are the irradiance and incidence angles, respectively, and

$$m = \frac{-\ln(2)}{\ln(\cos(\Phi_{1/2}))} \quad (2)$$

is the Lambertian emission order, where $\Phi_{1/2}$ is the transmitter semi-angle at half power. Finally $T(\psi_{i,j})$ denotes the optical filter gain, and

$$g(\psi_{i,j}) = \begin{cases} \frac{n_c^2}{\sin^2 \Psi_{\mathrm{FOV}}}, & 0 \le \psi_{i,j} \le \Psi_{\mathrm{FOV}} \\ 0, & \psi_{i,j} > \Psi_{\mathrm{FOV}}, \end{cases} \quad (3)$$

denotes the optical concentrator gain, where Ψ_{FOV} is the field-of-view of the transmitter and n_c is the refractive index.

The baseband equivalent received signal of user j at time instant t can be written as

$$y_j(t) = \eta \sum_{i \in \mathcal{I}} h_{i,j}\, I_i(t) + n(t), \quad (4)$$

where η is the responsivity of the photodetector and $I_i(t)$ is the instantaneous optical intensity emitted by the VLC AP with index i. In order to guarantee eye and device safety, I_i is constrained in terms of peak (i.e., $I_i(t) \le \mathcal{A}$) and average (i.e., $\mathbb{E}[I_i(t)] \le \mathcal{E} = \alpha\mathcal{A}$) intensity, where $\alpha = \frac{\mathcal{E}}{\mathcal{A}} \in [0, \frac{1}{2}]$. Also, $n(t)$ is the additive white Gaussian noise (AWGN) with zero mean and variance σ^2. It is noted that different sources of noise, such as thermal noise, ambient light shot noise, or relative intensity noise, are combined together within n.

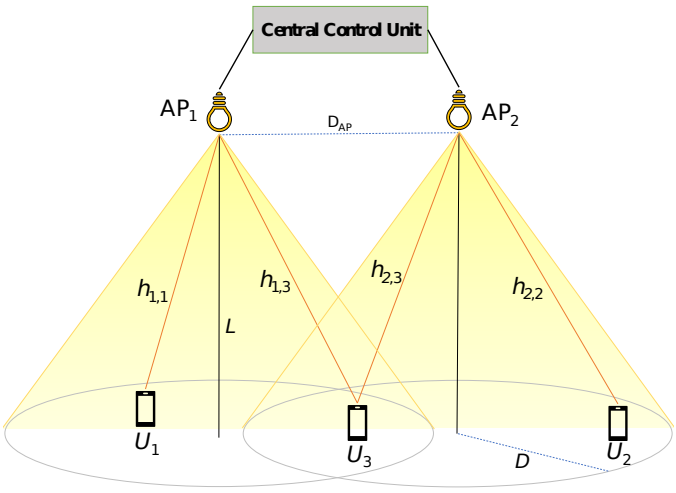

Fig. 1: System model for the 2-cell VLC system composed of two primary users (U_1 and U_2) and one secondary user (U_3).

More specifically, AP i transmits via the intensity modulation of its LED (I_i) a message that can be expressed as

$$\mathrm{X}_i^{\mathrm{LED}} = \sum_{j \in \mathcal{J}} \mathrm{X}_{i,j} \qquad i \in \mathcal{I}, \quad (5)$$

where $\mathrm{X}_{i,j}$ are independent data-carrying signals that AP i sends for user j. We define $\theta_{i,j} \in [0,1]$, with $\sum_{j \in \mathcal{J}} \theta_{i,j} = 1$, as the power splitting ratio that AP i allocates to the message intended to user j. As expected, in case user j is outside the coverage area of AP i, $\theta_{i,j} = 0$ for energy saving purposes. Thus, due to the average and peak illumination constraints that were set for eye-safety reasons, we must also verify that

$$\mathrm{X}_{i,j} \le \mathcal{A}_{i,j} = \theta_{i,j}\mathcal{A}, \qquad \mathbb{E}[\mathrm{X}_{i,j}] \le \mathcal{E}_{i,j} = \theta_{i,j}\mathcal{E}. \quad (6)$$

.

The received data-carrying signal for a target user with index $k \in \mathcal{J}$ can be then modeled as random variable, i.e.,

$$\begin{aligned} \mathrm{Y}_k &= \eta \sum_{i \in \mathcal{I}} h_{i,k} \left(\sum_{j \in \mathcal{J}} \mathrm{X}_{i,j} \right) + Z_k \\ &= \underbrace{\eta \sum_{i \in \mathcal{I}} h_{i,k}\, \mathrm{X}_{i,k}}_{\text{desired signal}} + \underbrace{\eta \sum_{i \in \mathcal{I}} h_{i,k} \left(\sum_{j \in \mathcal{J},\, j \neq k} \mathrm{X}_{i,j} \right)}_{\text{interference signal}} + \mathrm{Z}_k. \end{aligned} \quad (7)$$

Note that the index k is used to avoid confusion between the user j for whom the message is intended to, and the user k who decodes the message and it is not necessary the target destination. Also, the random variable Z_k represents $n(t)$ as independent of the transmit signals Gaussian random variable.

It is worth noticing that primary users is expected to decode up to 2 messages, while the secondary user may decode up to 4 messages. Thus, the average and peak constraints of a message $\mathrm{X}_{i,j}$ received from user k can be given from (6), replacing $(\eta h_{i,k})$ as $(\eta h_{i,k}\mathcal{A}_{i,j})$ and $(\eta h_{i,k}\mathcal{E}_{i,j})$, respectively.

In order to estimate the achievable rate of VLC channel that is described in (7), first we assume that our messages are all Truncated Gaussian (TG) [1] distributed and independent. Then we utilize the inner bound given in Lemma 4 from [14]. There, it is stated that a channel with a single desired TG distributed signal $\mathrm{X}_{i,k}$, experiencing interference from a sum of TG distributed signals $X_{i,j}$ $(j \in \mathcal{J})$ and zero-mean input-independent Gaussian noise Z_k, may achieve data rate

$$r^{(k)}_{\mathrm{X}_{i,k}|X_{i,j\in\mathcal{J}}} \geq \frac{1}{2}\log_2\left(\frac{\nu^2_{i,k}}{\widetilde{\nu}^2_{i,k}} + \frac{\nu^2_{i,k}}{\sum_{j\in\mathcal{J}}\widetilde{\nu}^2_{i,j}+\sigma^2}\right) - \phi$$
$$= \frac{1}{2}\log_2\left(1 + \frac{(\eta h_{i,k}\mathcal{E}_{i,k})^2(1+\epsilon_\mu)^{-2}}{\sum_{j\in\mathcal{J}}(\eta h_{i,k}\mathcal{E}_{i,j})^2 + 9\sigma^2}\right) - \epsilon_\phi, \quad (8)$$

where, equality holds by making the same assumptions as in [14]. It is noted that $X_{i,j}$ with $j \in \mathcal{J}$ denotes a signal treated as interference, while $\mathrm{X}_{i,k}$ is the desired signal intended to the target user k. The inner bound for the case that a message is decoded without interference is given by [15]

$$r^{(k)}_{X_{i,k}|\{\cdot\}} \geq \frac{1}{2}\log_2\left(1 + \frac{(\eta h_{i,k}\mathcal{E}_{i,k})^2}{9\sigma^2(1+\epsilon_\mu)^2}\right) - \epsilon_\phi. \quad (9)$$

Now that the mathematical formulation of the problem is ready from the information theory perspective, we can start working on the encoding and decoding algorithms to be implemented in the VLC APs (transmitter) and users (receiver), respectively.

III. MAC Scheduler

In this section, two methods for the MAC scheduler will be presented. In the first scheme, the messages $X_{1,3}$ and $X_{2,3}$ intended for the secondary user are assumed different and independent. In the second scheme, the two VLC APs (transmitters) encode the same codeword $\mathcal{W}$ to $\mathrm{X}_{1,3}$ and $\mathrm{X}_{2,3}$ and, due to that, they contain the same information verifying

$$\mathrm{X}_3 = \mathrm{X}_{1,3} + \mathrm{X}_{2,3} \quad (10)$$

with peak illumination constraint $\mathcal{A}_{1,3} + \mathcal{A}_{2,3}$ and average illumination constraint $\mathcal{E}_{1,3}+\mathcal{E}_{2,3}$, respectively. Note that in the first scheme, the secondary user (U_3) receives four messages in total, two of which are considered as interference, intended for the other two primary users (U_1, U_2), and the other remaining two messages that are part of the own messages coming from both APs. In the second scheme, the secondary user (U_3) receives three messages, two interfering messages and one common own message transmitted by both APs.

The proposed algorithm initializes by obtaining the position of all the (three) users and the QoS requirements of the (two) primary users. Then, the calculation of the optical wireless channel coefficients is carried out for all users with the aid of (1). In the next step, utilizing the CR-NOMA concept, power allocation factors $\theta_{i,j}$ are chosen in order to satisfy the QoS constraints of the primary users served by each of the VLC APs. For this purpose, we define a sequence index $s_l \in \mathcal{S}$, where each value corresponds to a specific case concerning the decoding order of the primary users as follows:

$$\mathcal{S} \triangleq \begin{cases} \mathrm{s}_1, & U_1 \text{ and } U_2 \text{ decode their messages first} \\ \mathrm{s}_2, & U_1 \text{ and } U_2 \text{ decode their messages second} \\ \mathrm{s}_3, & U_1 \text{ decodes first and } U_2 \text{ decodes second} \\ \mathrm{s}_4, & U_2 \text{ decodes first and } U_1 \text{ decodes second} \end{cases}. \quad (11)$$

Consider that the power splitting ratio $\theta_{i,j}$ can be found with the aid of both (8) and (9), depending on the decoding order. Then, setting $r^{(j)}_{\mathrm{X}_{i,j}|\mathrm{X}_{i,3}}$ equal to the target data rate $\mathcal{R}_j$, and considering that $\theta_{i,j\neq 3} \triangleq \sum_{j\in\mathcal{J},j\neq 3}\theta_{i,j} = 1-\theta_{i,3}$, it is possible to observe after few mathematical manipulations that

$$\theta^2_{i,j} - \frac{2A}{A-1}\theta_{i,j} + \frac{A(B+1)}{A-1} = 0, \quad (12)$$

where $A = \left(2^{2(\mathcal{R}_j+\epsilon_\phi)}-1\right)(1+\epsilon_\mu)^2$ and $B = \frac{9\sigma^2}{(\eta h_{i,j}\mathcal{E})^2}$. Let $\theta^{(1)}_{i,j}$ and $\theta^{(2)}_{i,j}$ denote the solutions of (12). Then, we hold as accepted solution that

$$\widetilde{\theta}_{i,j} = \left[\min\{\theta^{(1)}_{i,j}, \theta^{(2)}_{i,j}, 1\}\right]^+, \quad (13)$$

where $[.]^+$ denotes the $\max\{\cdot, 0\}$ operation. Also, for the case in which the primary user decodes its desired message second after performing SIC, the right part of (9) is now set equal to $\mathcal{R}_j$. The solution $\widetilde{\theta}_{i,j}$ of the resulting equation can be written as a function of the previously defined A and B, i.e.,

$$\widetilde{\theta}_{i,j} = \sqrt{AB}, \quad (14)$$

where the negative solution is rejected because $\theta_{i,j} \in [0,1]$. In this case, we also have to determine the achievable rate such

Algorithm 1: Decoding Algorithm (Scheme 1)

Input: $h_{i\in\mathcal{I},j\in\mathcal{J}}$, $\mathcal{R}_1$, $\mathcal{R}_2$
for all $s_l \in \mathcal{S}$ **do**
  Find $\widetilde{\theta}_{i,j}$ via (13) or (14)
  Find r_j via (15)
  Determine R_3 using O_1
  Determine R_3 using O_2
  if U_3 cannot extract any interference using either O_1 or O_2 **then**
    if $r^{(3)}_{\mathrm{X}_{1,3}|\mathrm{X}_{2,3},\mathrm{X}_{1,1},\mathrm{X}_{2,2}} \geq r^{(3)}_{\mathrm{X}_{2,3}|\mathrm{X}_{1,3},\mathrm{X}_{1,1},\mathrm{X}_{2,2}}$ **then**
      Determine R_3 using O_3 with $i=1$
    else
      Determine R_3 using O_3 with $i=2$
    end if
  end if
  Hold maximum R_3 determined.
end for
Hold maximum R_3.

[1]The definition of the Truncated Gaussian distribution can be found in [13], where it was proven that truncated exponential distributions maximize the mutual information in order to find the capacity of an (IM) optical channel.

that a primary user (i.e., U_1 or U_2) can decode correctly the message intended to the secondary user (i.e., U_3). This inner bound is derived from (8), i.e.,

$$r_j = r^{(j)}_{X_{i,3}|X_{i,j}} \qquad \text{for } j = 1, 2. \tag{15}$$

For the next step, given the power splitting ratios values $\theta_{i,j}$ of the primary users, which correspond to a predefined decoding sequence s_l, we must determine whether the secondary user can remove the interference generated by the messages intended for the primary users or not. For this purpose, we first define the set of policies $\mathcal{O} \triangleq \{O_1, O_2, O_3\}$ as follows:

$$\mathcal{O} = \begin{cases} O_1, & U_1 \to U_2 \to U_3 \\ O_2, & U_2 \to U_1 \to U_3 \\ O_3(i), & U_{i,3} \stackrel{\to}{} O_1 \text{ or } O_2 \end{cases}. \tag{16}$$

where three policies are introduced. These three policies indicate the decoding sequence that the secondary user (U_3) will follow in order to decode its desired message(s). O_1 and O_2 are similar, due to the fact that U_3 tries to extract the interference from both primary users before decoding its desired message(s). $O_3(i)$ is a special policy, where U_3 first decodes its desired message from AP i and, then, utilizes either O_1 or O_2 to decode its desired message from the other AP. $O_3(i)$ is not considered when both APs send the same message. It is important to note that regardless the policy in set $\mathcal{O}$ that is utilized, the SIC procedure stops when the user cannot remove the interference (from a message intended to another user) in the given order. In this situation, the target user decode its desired messages assuming that those messages that were not removed behave as interference. In Scheme 1, before beginning the sequential decoding of the own message(s), it also needs to be checked which of the desired messages achieves a better rate while treating the others as interference. For a better understanding of all the above we refer to algorithm 2, where the procedure for determining R_3 is presented utilizing transmission Scheme 1 and following policy O_1.

When Scheme 2 is implemented, the less complex Algorithm 3 is utilized. After constructing signal X_3 and its constraints, the appropriate replacements in (8) are needed to check what are the messages that the secondary user (U_3) can decode, and to determine the value of R_3 via O_1 and O_2.

Algorithm 2: Illustrative example of policy O_1

Input: $h_{i,3}$, $\widetilde{\theta}_{i,j}$, r_j, $\mathcal{R}_j$

if $r^{(3)}_{X_{1,1}|X_{1,3},X_{2,3},X_{2,2}} \geq \mathcal{R}_1$ **then**
  if $r^{(3)}_{X_{2,2}|X_{1,3},X_{2,3}} \geq \mathcal{R}_2$ **then**
    if $r^{(3)}_{X_{1,3}|X_{2,3}} \geq r^{(3)}_{X_{1,3}|X_{2,3}}$ **then**
      $R_3 = \min\{r^{(3)}_{X_{1,3}|0}, r_1\} + \min\{r^{(3)}_{X_{2,3}|X_{1,3}}, r_2\}$;
    else
      $R_3 = \min\{r^{(3)}_{X_{1,3}|X_{2,3}}, r_1\} + \min\{r^{(3)}_{X_{2,3}|0}, r_2\}$;
    end if
  else
    if $r^{(3)}_{X_{1,3}|X_{2,3},X_{2,2}} \geq r^{(3)}_{X_{1,3}|X_{2,3},X_{2,2}}$ **then**
      $R_3 = \min\{r^{(3)}_{X_{1,3}|X_{2,2}}, r_1\} + \min\{r^{(3)}_{X_{2,3}|X_{1,3},X_{2,2}}, r_2\}$;
    else
      $R_3 = \min\{r^{(3)}_{X_{1,3}|X_{2,3},X_{2,2}}, r_1\} + \min\{r^{(3)}_{X_{2,3}|X_{2,2}}, r_2\}$;
    end if
  end if
else
  if $r^{(3)}_{X_{1,3}|X_{2,3},X_{2,2},X_{1,1}} \geq r^{(3)}_{X_{1,3}|X_{2,3},X_{2,2},X_{1,1}}$ **then**
    $R_3 = \min\{r^{(3)}_{X_{1,3}|X_{2,2},X_{1,1}}, r_1\} + \min\{r^{(3)}_{X_{2,3}|X_{1,3},X_{2,2},X_{1,1}}, r_2\}$;
  else
    $R_3 = \min\{r^{(3)}_{X_{1,3}|X_{2,3},X_{2,2},X_{1,1}}, r_1\} + \min\{r^{(3)}_{X_{2,3}|X_{2,2},X_{1,1}}, r_2\}$;
  end if
end if

Output: R_3

Algorithm 3: Decoding Algorithm (Scheme 2)

Input: $h_{i\in\mathcal{I},j\in\mathcal{J}}$, $\mathcal{R}_j$;
1: Find $\widetilde{\theta}_{i,j}$ via (13) or (14);
2: Find r_j via (15)
3: Determine R_3 using O_1;
4: Determine R_3 using O_2;
Output: Hold maximum R_3 determined;

IV. Simulation Parameters and Numerical Results

In this section, Monte Carlo simulation results assuming 10^5 instances (snapshots) are presented and discussed in detail, in order to give further insight on the VLC network performance. First of all, Table I lists the values of the parameters used for the simulations, which correspond to practical values of a VLC system. It is noted that the cell radius D is given as function of Ψ_C and L, due to the geometric approach of the problem, and is assumed identical for both VLC APs (cells). This radius corresponds to circles, which represent the plane of the receiver in which the photodiodes are located.

In Fig. 2, the data rate of the secondary user (R_3) is presented for various cell-center Signal-to-Noise Ratio (SNR) values, $\mathrm{SNR} = (\eta h_0 \mathcal{E})^2/\sigma^2$, where h_0 is the VLC channel gain when the receiver is directly below the AP (i.e., aligned with the boresight direction of the LED). It can be shown that the first of the two proposed practical protocols achieves slightly higher performance. On top of that, these protocols are compared with a benchmark scheme, where the two APs send the same information to secondary user, but this user is not able to perform SIC [16]. The superiority of the proposed schemes over the benchmark approach is clearly observed, especially when the QoS constraint of the primary users takes moderate values. It is noted that for this figure, the distance between the APs is given as $D + 0.3$; moreover, in this situation, the QoS requirement of the primary users can be expressed as $\mathcal{R}_j = \mathrm{R}^{\mathrm{thr}}$, without loss of generality.

The impact of the distance between the two APs is evaluated

TABLE I: Simulation Parameters of the downlink VLC system

Parameter	Value	Parameter	Value
$T(\psi_i)$	1	Ψ_C	$\pi/3$
L	2.15 m	$\Phi_{1/2}$	$\pi/3$
n	1.5	A_r	1 cm^2
η	0.5 A/W	D	$L\tan(\Psi_C)$

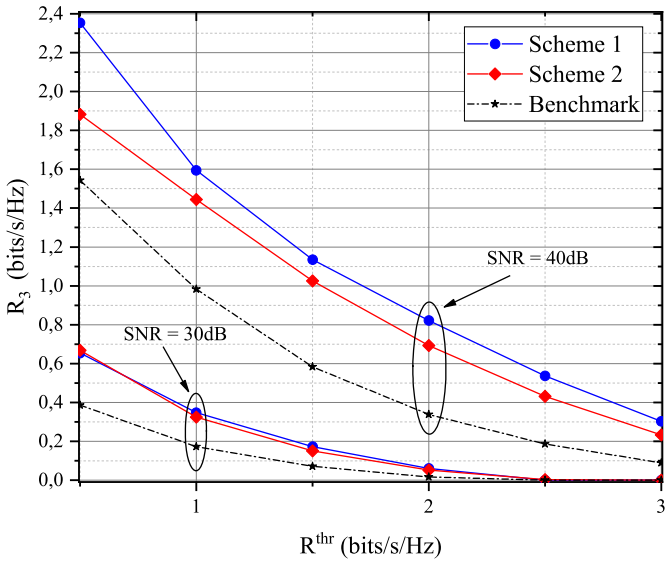

Fig. 2: Data rate of the secondary user (R_3) as function of the QoS constraints of the primary users (R^{thr}) for the two schemes under analysis.

in Fig. 3. The values of distance that were considered in the simulation setup extended, in this case, from 4 to 6 meters. The primary users had both a QoS requirement of $\mathcal{R}_j$ =1 bit/s/Hz. The simulations were performed for two different values of cell-center SNR. Interestingly, based on the obtained simulation results reported in this figure, larger distances between the APs made Scheme 2 outperform Scheme 1. This result recommends to design of VLC networks implementing Scheme 2 when APs are located relatively far away. Note that in addition to better performance, Scheme 2 demands less complexity as a lower number of SIC operations are needed.

The data rate of the secondary user (R_3) as function of cell-center SNR is shown in Fig. 4. In this figure, the distance between the APs is set equal to $D + 0.3$ meters, while two settings for R^{thr} are considered. It is very interesting to observe that for higher QoS requirements, there is a higher gain of Scheme 1 over Scheme 2 for medium to high cell-center SNR values. This is a benefit due to the greater degree of freedom offered by sending two different messages.

V. Conclusion

This paper considered a distributed NOMA VLC network with a unified MAC scheduler, aiming at dealing with the strong inter-cell interference power that is representative of such ultra-dense network deployments. Two practical protocols were proposed and evaluated, providing a performance that

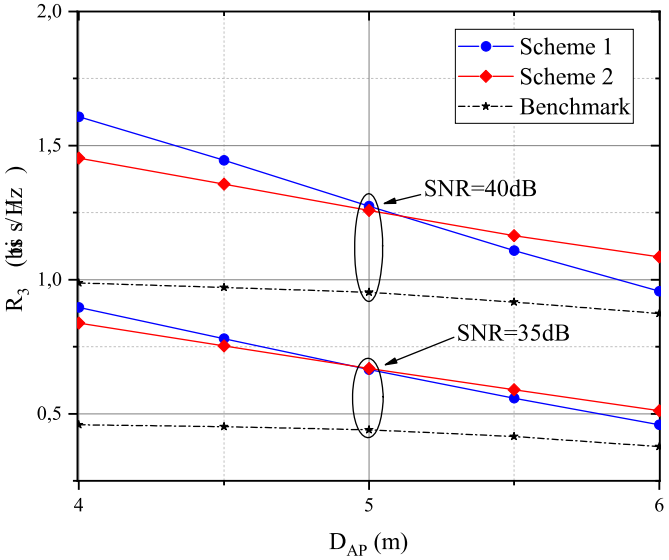

Fig. 3: Data rate of the secondary user (R_3) as function of the separation distance between VLC APs (D_{AP}).

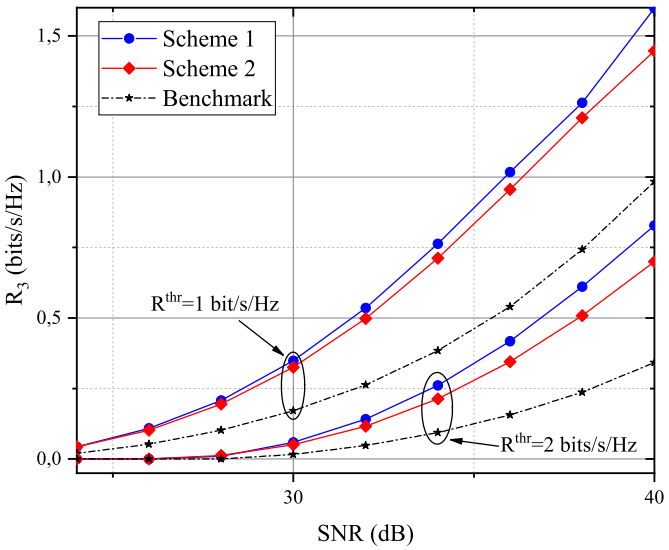

Fig. 4: Data rate of the secondary user (R_3) as function of the cell-center SNR.

was very similar between them. However, when compared to the performance of the benchmark approach used in conventional cellular schemes that employ NOMA, the outcome of the new proposed schemes was much better. Given the particularities of the VLC network and the received message of each user, the decoding strategy that needs to be followed was not as obvious as in the power domain NOMA. Therefore, the proposed MAC scheduler took into account the optimal decoding order and power allocation factors in the given VLC setting, maximizing the spectral efficiency of a cell-edge (secondary) user while simultaneously securing the QoS constraints of the cell-center (primary) users.

ACKNOWLEDGMENT

This paper is based upon work from COST Action CA19111 (European Network on Future Generation Optical Wireless Communication Technologies, NEWFOCUS), supported by COST (European Cooperation in Science and Technology).

REFERENCES

[1] O. Maraqa, A. S. Rajasekaran, S. Al-Ahmadi, H. Yanikomeroglu, and S. M. Sait, "A Survey of Rate-Optimal Power Domain NOMA With Enabling Technologies of Future Wireless Networks," *IEEE Commun. Surveys Tuts.*, vol. 22, no. 4, pp. 2192–2235, 2020.

[2] K. G. Rallis, V. K. Papanikolaou, P. D. Diamantoulakis, M.-A. Khalighi, and G. K. Karagiannidis, "Energy Efficiency Maximization in Cooperative Hybrid VLC/RF Networks with NOMA," in *Proc. 17th Int. Symp. Wireless Commun. Syst. (ISWCS)*, Berlin, Germany, Sep. 2021, pp. 1–6.

[3] Z. Ding, X. Lei, G. K. Karagiannidis, R. Schober, J. Yuan, and V. K. Bhargava, "A Survey on Non-Orthogonal Multiple Access for 5G Networks: Research Challenges and Future Trends," *IEEE J. Select. Areas Commun.*, vol. 35, no. 10, pp. 2181–2195, 2017.

[4] M. Wafik Eltokhey, M.-A. Khalighi, and Z. Ghassemlooy, "Power Allocation Optimization in NOMA-Based Multi-Cell VLC Networks," in *Proc. 17th Int. Symp. Wireless Commun. Syst. (ISWCS)*, 2021, pp. 1–5.

[5] H. Kazemi and H. Haas, "Downlink cooperation with fractional frequency reuse in DCO-OFDMA optical attocell networks," in *Proc. IEEE Int. Conf. Commun (ICC)*, 2016, pp. 1–6.

[6] A. Ibrahim, T. Ismail, K. F. Elsayed, M. S. Darweesh, and J. Prat, "Resource Allocation and Interference Management Techniques for OFDM-Based VLC Atto-Cells," *IEEE Access*, vol. 8, pp. 127 431–127 439, 2020.

[7] V. Van Huynh, N.-T. Le, N. Saha, M. Z. Chowdhury, and Y. M. Jang, "Inter-cell interference mitigation using soft frequency reuse with two FOVs in visible light communication," in *Proc. Int. Conf. ICT Convergence (ICTC)*, 2012, pp. 141–144.

[8] A. Dowhuszko and A. Pérez-Neira, "Achievable data rate of coordinated multi-point transmission for visible light communications," in *Proc. IEEE Annu. Int. Symp. Personal, Indoor, and Mobile Radio Commun. (PIMRC)*, Oct. 2017, pp. 1–7.

[9] Y. Tian, A. R. Nix, and M. Beach, "On the Performance of Opportunistic NOMA in Downlink CoMP Networks," *IEEE Commun. Lett.*, vol. 20, no. 5, pp. 998–1001, 2016.

[10] M. S. Ali, E. Hossain, A. Al-Dweik, and D. I. Kim, "Downlink Power Allocation for CoMP-NOMA in Multi-Cell Networks," *IEEE Trans. Commun.*, vol. 66, no. 9, pp. 3982–3998, 2018.

[11] A. Kilzi, J. Farah, C. Abdel Nour, and C. Douillard, "Mutual Successive Interference Cancellation Strategies in NOMA for Enhancing the Spectral Efficiency of CoMP Systems," *IEEE Trans. Commun.*, vol. 68, no. 2, pp. 1213–1226, 2020.

[12] P. D. Diamantoulakis and G. K. Karagiannidis, "Performance Analysis of Distributed Uplink NOMA," *IEEE Commun. Lett.*, vol. 25, no. 3, pp. 788–792, 2021.

[13] A. Chaaban, Z. Rezki, and M.-S. Alouini, "On the Capacity of Intensity-Modulation Direct-Detection Gaussian Optical Wireless Communication Channels: A Tutorial," *IEEE Commun. Surveys Tuts.*, pp. 1–1, 2021.

[14] A. Chaaban, O. M. S. Al-Ebraheemy, T. Y. Al-Naffouri, and M.-S. Alouini, "Capacity Bounds for the Gaussian IM-DD Optical Multiple-Access Channel," *IEEE Trans. Wireless Commun.*, vol. 16, no. 5, pp. 3328–3340, 2017.

[15] A. Chaaban, Z. Rezki, and M.-S. Alouini, "On the Capacity of the Intensity-Modulation Direct-Detection Optical Broadcast Channel," *IEEE Trans. Wireless Commun.*, vol. 15, no. 5, pp. 3114–3130, 2016.

[16] S. Fayad, M. A. Arfaoui, A. Ghrayeb, and C. Assi, "CoMP Transmission in Downlink NOMA-Based Indoor VLC Cellular Systems," 2021. [Online]. Available: https://arxiv.org/abs/2108.02361